



Targeting neratinib-induced diarrhea with budesonide and colesevelam in a rat model

Kate R. Secombe¹ · Imogen A. Ball¹ · Joseph Shirren¹ · Anthony D. Wignall¹ · John Finnie² · Dorothy Keefe¹ · Francesca Avogadri-Connors³ · Elizabeth Olek³ · David Martin³ · Susan Moran³ · Joanne M. Bowen¹

Received: 31 July 2018 / Accepted: 4 December 2018 / Published online: 10 December 2018
© Springer-Verlag GmbH Germany, part of Springer Nature 2018

Abstract

Purpose Neratinib is an irreversible pan-ErbB tyrosine kinase inhibitor used for the extended adjuvant treatment of early-stage HER2-positive breast cancer. Its use is associated with the development of severe diarrhea in up to 40% of patients in the absence of proactive management. We previously developed a rat model of neratinib-induced diarrhea and found inflammation and anatomical disruption in the ileum and colon. Here we tested whether anti-diarrheal interventions, budesonide and colesevelam, can reduce neratinib-induced diarrhea and intestinal pathology.

Methods Rats were treated with 50 mg/kg neratinib via oral gavage for 14 or 28 days (total $n = 64$). Body weight and diarrhea severity were recorded daily. Apoptosis was measured using immunohistochemistry for caspase-3. Inflammation was measured via a multiplex cytokine/chemokine assay. ErbB levels were measured using PCR and Western Blot.

Results Budesonide co-treatment caused rats to gain significantly less weight than neratinib alone from day 4 of treatment ($P = 0.0418$). Budesonide ($P = 0.027$) and colesevelam ($P = 0.033$) each reduced the amount of days with moderate diarrhea compared to neratinib alone. In the proximal colon, rats treated with neratinib had higher levels of apoptosis compared to controls ($P = 0.0035$). Budesonide reduced histopathological injury in the proximal ($P = 0.0401$) and distal colon ($P = 0.027$) and increased anti-inflammatory IL-4 tissue concentration (ileum; $P = 0.0026$, colon; $P = 0.031$) compared to rats treated with neratinib alone. In the distal ileum, while budesonide decreased ErbB1 mRNA expression compared to controls ($P = 0.018$) (PCR), an increase in total ErbB1 protein was detected ($P = 0.0021$) (Western Blot).

Conclusion Both budesonide and colesevelam show potential as effective interventions against neratinib-induced diarrhea.

Keywords Targeted therapies · Diarrhea · Breast cancer · Rat model · Neratinib

Introduction

Neratinib (PB272) is an orally available, high affinity, irreversible small molecule pan-ErbB tyrosine kinase inhibitor (TKI). It has been FDA approved for extended adjuvant

treatment of early-stage HER2+ breast cancer and is being evaluated clinically in other HER2-driven cancers. High level expression of HER2 protein is a well-established oncogenic driver in approximately 20% of breast cancers [1]. Neratinib has shown encouraging results in metastatic and early-breast cancer settings, and also when given to patients who have previously received trastuzumab treatment [2].

Members of the ErbB family are expressed on the cell membrane of cancer cells as well as being widely expressed on gastrointestinal epithelial cells, and have various functions such as cell proliferation and regulation of intestinal epithelial cell apoptosis [3]. The activity of neratinib occurs due to its covalent binding to a cysteine residue at the adenosine triphosphate binding site that is highly conserved across the ErbB family members ERBB1, 2 and 4. This covalent bond with the cysteine residue prevents receptor phosphorylation

Electronic supplementary material The online version of this article (<https://doi.org/10.1007/s00280-018-3756-8>) contains supplementary material, which is available to authorized users.

✉ Kate R. Secombe
kate.secombe@adelaide.edu.au

¹ Adelaide Medical School, University of Adelaide, Level 2 Helen Mayo Building South, Frome Rd, Adelaide, South Australia 5005, Australia

² SA Pathology, Adelaide, South Australia, Australia

³ Puma Biotechnology Inc, Los Angeles, CA, USA

causing permanent blockade of the tyrosine kinase activity and downstream signaling.

Diarrhea has been a prominent adverse effect in most clinical trials for neratinib. Most grade 3 diarrhea occurrences happen in the first month of treatment, with a reduction in frequency thereafter [1]. In the ExteNET trial of 2840 women with breast cancer randomized to 12 months of treatment with oral neratinib or placebo, 40% of neratinib-treated patients developed severe, grade 3–4 diarrhea. Grade 1 and 2 diarrhea occurred in 55% of neratinib patients in a setting where no mandatory diarrhea prophylaxis was given, as was the case in ExteNET [4]. A recent review highlighted that in studies without mandatory diarrhea management, 30–53% of patients experience grade 3 diarrhea following neratinib [3].

Prophylactic loperamide has decreased diarrhea incidence in some cases. The I-SPY 2 trial showed that introducing a lower dose intensity prophylactic regimen of loperamide in the treatment protocol modestly decreased severe diarrhea from 47 to 36% in patients receiving neoadjuvant neratinib plus chemotherapy for breast cancer [5]. Interim results from the Phase 2 CONTROL study of women with early-stage HER2+ breast cancer receiving extended adjuvant neratinib showed that the incidence of grade 3 diarrhea was 30.7% in patients receiving loperamide prophylaxis, however, the median number of grade 3 diarrhea episodes per patient was 1 and the median cumulative duration of grade 3 diarrhea was 3 days [6]. However, loperamide has side effects including unwanted cardiac effects, fatigue, constipation, abdominal pain and dizziness [7–9]. Thus, a gap remains for attaining the most effective diarrhea management approach. As such, we utilized our established rat model to determine the underlying mechanisms of neratinib-induced diarrhea, to more effectively target possible interventions.

In this study, we tested budesonide, a potent locally acting corticosteroid used for inflammatory gastrointestinal conditions, and colestevlam, a bile acid sequestrant, to target intestinal changes associated with neratinib diarrhea. Budesonide is an agonist of glucocorticoid receptors with high topical anti-inflammatory activity and low systemic bioavailability. Budesonide has previously decreased diarrhea in chemotherapy-induced diarrhea and Crohn's disease [10–13]. Colestevlam hydrochloride is an orally administered bile acid sequestrant, FDA approved for lipid lowering, but also used off label to treat bile acid malabsorption and subsequent diarrhea. Previous studies have shown that colestevlam can cause reduction of diarrhea in Crohn's disease patients [14] which may have overlapping features with neratinib-induced changes in the small intestine.

Materials and methods

Chemicals and reagents

Neratinib was kindly provided by Puma Biotechnology (USA). Neratinib was administered at 50 mg/kg, diluted in 0.5% (w/w) hydroxypropyl methylcellulose buffer. Budesonide (Sigma-Aldrich, USA) was administered at 1 mg/kg, with dimethyl sulfoxide (DMSO)/1% carboxymethyl cellulose buffer (CMC) 1:99 vehicle. Colestevlam (Welchol, Daiichi Sankyo, USA) was suspended in MilliQ water at a concentration of 300 mg/kg.

Animals and ethics

All experiments were conducted in male Albino Wistar (AW) rats obtained from the University of Adelaide Laboratory Animal Service. These rats respond to small molecule receptor tyrosine kinase inhibitors with clinically relevant diarrhea [15]. Rats were housed in groups of up to four in individually ventilated cages. The environmental controls were set to maintain temperature within the range of 19–23 °C and relative humidity within the range of 45–65%; with a 12-h light/dark cycle. Rodent chow and water were available ad libitum. If rats were experiencing moderate to severe treatment-related toxicity (e.g., diarrhea, weight loss, stress markings) they were allowed soaked chow in addition. Rats were acclimatized to local housing conditions for a minimum of 7 days prior to the first day of dosing. On Day 1 of treatment, the rats were between 7 and 9 weeks old. This study was approved by the Animal Ethics Committee of the University of Adelaide, and complied with the National Health and Medical Research Council (Australia) Code of Practice for Animal Care in Research and Training (2014).

Experimental design

For each experiment, all rats were randomly allocated to experimental groups ($n=7-9$ per group). Rats were identified by a unique animal number written with an indelible marker on their tail. During the 28-day treatment period, rats received daily oral gavages using a soft plastic feeding tube. Neratinib, intervention or vehicle were given at a constant dose volume of approximately 5 mL/kg unless otherwise shown. Individual dose volumes were adjusted daily according to most recent body weight. The first day of dosing was designated Day 1. The final dose was given on the day before scheduled necropsy. The terminal necropsy was conducted on Days 15 or 29 which reflected 14 and 28 days of receiving neratinib, respectively. This treatment design mimics the long term continuous administration in clinical trials and

also allows examination of sub-acute and chronic damage. All rats were anesthetized via isoflurane inhalation, and then culled by cardiac exsanguination and cervical dislocation.

Clinical gut toxicity assessment

Rats were weighed daily, and there was a twice daily comprehensive clinical symptom recording. Diarrhea was graded by two assessors according to an established grading system [15]. Briefly, there were four grades: 0, no diarrhea; 1, mild (soft unformed stools); 2, moderate (perianal staining and loose stools); 3, severe (watery stools and staining over legs and abdomen). Rats were euthanized if they displayed $\geq 15\%$ weight loss or significant distress and clinical deterioration, in compliance with animal ethical requirements.

Tissue collection and preparation

At necropsy, the gastrointestinal tract was removed from the pyloric sphincter to the rectum. The small and large intestine were flushed with chilled, sterile PBS and weighed. Samples of duodenum, jejunum, and proximal and distal ileum and colon were collected and fixed in 10% formalin for embedding in paraffin. Other organs (stomach, spleen, liver, brain, kidney, lungs, heart, and digestive tract) were also collected, weighed, fixed in formalin and embedded in paraffin. Mucosal scrapings from jejunum, ileum and colon were collected and stored in RNAlater (Sigma-Aldrich) for preservation of mRNA.

Serum analysis

Serum samples for blood biochemistry were taken by cardiac puncture at time of necropsy. Serum was separated by centrifugation at 300 g for 5 min before being analyzed via a multiple blood analysis (MBA-20). This analysis was completed by the Department of Clinical Pathology, SA Pathology, Adelaide, South Australia.

For serum neratinib concentration analysis, blood samples were collected from a tail vein before dosing on day 8, 15, 22, and 29 of treatment. Serum neratinib concentration was measured by liquid chromatography–tandem mass spectrometry (LC–MS) (validated range 10–10,000 ng/ml). This work was conducted in the Pharmaceutical Science Sector Laboratory, School of Pharmacy and Medical Sciences, University of South Australia under GLP conditions. Calibrator and quality control working control solutions were prepared by dissolving neratinib in methanol. Sample supernatant was aspirated and eluted through a Phenomenex Kinetex 1.7 μm C18 2.1 \times 100 mm column using a Shimadzu 30 series UHPLC system.

Histological examination

All histology was conducted on paraffin embedded intestinal samples, which were cut using a rotary microtome and 4 μm sections mounted onto Superfrost glass slides (Menzel-Glaser, Germany). All histology had images taken using a NanoZoomer digital slide scanner (Hamamatsu Photonics, Japan) and viewed using the NanoZoomer Digital Pathology Software (NDP View v1.2) (Histalim, France). Routine hematoxylin and eosin staining was completed and an injury score assigned using a validated system of histological criteria [16, 17]. Criteria were villus fusion, villus atrophy, disruption of brush border and surface enterocytes, crypt losses/architectural disruption, disruption of crypt cells, infiltration of polymorphonuclear cells and lymphocytes, dilation of lymphatics and capillaries and edema. The latter six criteria were examined in the colon. Each criterion was scored in a blinded fashion as either present = 1 or absent = 0.

Immunohistochemistry

Immunohistochemical analysis was performed for apoptosis (ab4051, cleaved caspase-3, Abcam, Australia) and phosphorylated ErbB2 (ab101229, anti-ErbB2 phospho Y1248, Abcam, Australia). Analysis was performed using an automated stainer (Autostainer Plus, Dako, Denmark) using Dako reagents. Briefly, sections were mounted in specialized FLEX IHC microscope slides (Flex Plus detection system, Dako, #K8020). These sections were dewaxed in histolene and then rehydrated through graded ethanols. Heat-mediated antigen retrieval used an EDTA/Tris buffer (0.37 g/L EDTA, 1.21 g/L Tris, pH = 9.0). The retrieval buffer was preheated to 65 °C using the Dako PT LINK (pre-treatment module, Dako, #PT101). Slides were immersed in the buffer, which was then heated to 97 °C for 20 min. Once the buffer had cooled to 65 °C, slides were removed and placed in the Dako Autostainer Plus and stained following manufacturer supplied protocols. Negative controls had primary antibody omitted. Caspase-3-dependent apoptosis activity was quantified by dividing the number of positively stained cells by the number of crypts in 15 fields of view at 20 \times magnification. Data have been presented as average positively stained cells per crypt.

Western blot of ErbB1, pErbB1

Protein was extracted from full-thickness ileal and colonic tissue samples treated for 28 days. Tissue samples (30 mg) were immersed in 250 μL of RIPA buffer (Sigma-Aldrich, #R0278). Samples were homogenized using the Qiagen-Tissue Lyser LT at 50 Hz for 5 min. Homogenates were centrifuged at 10,000 $\times g$ for 15 min at 4 °C. Supernatant was then collected and aliquoted. The Pierce BCA protein

quantification kit (ThermoFisher Scientific, #23225) was used to quantify total protein relative to standard curve.

30 μg of protein lysate was supplemented with 4 μL of Bolt reducing agent (ThermoFisher Scientific, USA; #B0008) and 10 μL Bolt lithium dodecyl sulfate (LDS) sample buffer (ThermoFisher Scientific; #B0007). Total volume was adjusted to 40 μL with MilliQ water. Once samples had been denatured for 10 min at 70 $^{\circ}\text{C}$, they were loaded onto a precast Bolt 4–12% Bis–Tris Plus, SDS-PAGE Gels (12-well) (Thermo-Fisher Scientific; #NW04122BOX). Samples were separated using the Bolt mini gel tank at 200 V for 22 min. Proteins were transferred to a polyvinylidene difluoride membrane using the iBlot transfer stacks (ThermoFisher Scientific; #IB24002) and compatible iBlot 2 gel transfer device (ThermoFisher Scientific; #IB21001).

The membrane was washed with Tris-buffered saline and stained with Ponceau Red to confirm loading. The membrane was blocked and probed with primary and secondary antibodies using the iBind western device (ThermoFisher Scientific; #SLF1000) as per manufacturer's guidelines. Western blots were assessed using ImageStudio Lite, version 4.0 (Li-Cor Sciences, USA). Signal intensity was determined relative to local background. Data were presented normalized to the housekeeping gene Beta-actin (ab8227, Abcam, dilution = 1/800) and vehicle-treated controls.

Antibody details are as follows: anti-pErbB1 [Y1068] (ab5644, Abcam, dilution = 1/200) and anti-ErbB1 (ab15669, Abcam, dilution = 1/250). To confirm specificity of the ErbB1 protein, we used a recombinant rat ErbB1 protein (His Tag) (80100-R08H, Sino Biological, USA).

RT-PCR

Intestinal expression of ErbB1, ErbB2, ErbB4 and epithelial sodium channel gamma (ENaC- γ) was assessed using SYBR green-based real time PCR. Total RNA was isolated from mucosal scrapings from the ileum and colon. mRNA was purified using the Nucleospin mRNA purification RNA II kit (Macherey–Nagel, Germany) following the manufacturer's protocol. RNA (100 ng) was reverse transcribed using iScript cDNA synthesis kit (Bio-Rad, USA). cDNA was quantified and diluted to a working concentration of 100 ng/ μL . Primers were designed using web-based primer design program Primer 3, version 4. Genes of interest were ErbB1 (forward: 5'-CCCACAGCAAGGCTTCTTCA; reverse: 5'-CACCGCAGCTCCCATTTCTA), ErbB2 (forward: 5'-AACCTTTCCTTGCTGCTTGA; reverse: 5'-GTTCCCTCCAGACCTCTTCC), ErbB4 (forward: 5'-TGATTG CAGCCGGAGTCAT; reverse: 5'-TGACATAAACGGCAA ATGTCAGA) and ENaC- γ (forward: 5'-TCACGCTTTTCC ACCATCCA; reverse: 5'-GATGACTTGCAGCCCGTACT). ErbB1 and ErbB2 were denatured at 95 $^{\circ}\text{C}$ for 10 s, annealed at 54 $^{\circ}\text{C}$ for 15 s, and extended at 72 $^{\circ}\text{C}$ for 20 s (45 cycles),

followed by a melt curve analysis. ErbB4 was denatured at 95 $^{\circ}\text{C}$ for 15 s, annealed at 60 $^{\circ}\text{C}$ for 30 s and extended at 72 $^{\circ}\text{C}$ for 60 s. ENaC- γ used a one minute 60 $^{\circ}\text{C}$ anneal and extension phase. SYBR Green (Quantitect, Qiagen, Germany) was used to detect amplification using a Rotor-Gene Q (Qiagen, Germany). All reactions were completed in triplicate with normalization against the housekeeping gene UBC (forward: 5'-TCGTACCTTTCTCACCACAGTATC TAG, reverse: 5'-GAAAACCTAAGACACCTCCCCATCA).

Tissue cytokine quantification

To further understand the mechanism of budesonide-induced protection, cytokine concentration was measured in homogenates from the distal ileum and proximal colon (28 day groups) using Luminex xMAP (Milliplex MAP Kit rat cytokine/chemokine magnetic bead assay, Merck Millipore, USA). This kit was used as per manufacturer's instructions to analyze IL-4, IL-1 β , IL-10, IFN- γ , IL-17 α , MCP-1 and TNF- α . Each 96-well plate had a 6-point standard curve and two manufacturer-provided quality controls.

Fecal bile acid assay

To examine the effect of colessevelam on bile acid absorption, total bile acids were measured in fecal samples from vehicle control, neratinib only and neratinib + colessevelam rats. As rats were group housed, total bile acids were measured in pooled fecal samples collected over 8 h. Samples were prepared as per Boue et al. [18] and then assayed using the Crystal Chem rat total bile acid kit (USA) according to manufacturer's instructions.

Statistical analysis

Data were compared using Prism version 7.0 (GraphPad Software, USA). Test article groups were compared with the vehicle control group and neratinib alone group as indicated. Error bars on graphs are SEM. The assumptions of equality of variance for each group and normally distributed data were tested using Bartlett's test and D'Agostino & Pearson omnibus normality test, respectively. If these assumptions were violated, non-parametric equivalent tests were performed, including Kruskal–Wallis for independent data and Freidman's test for repeated measures. When assumptions held, analysis of variance tests (ANOVAs) were performed using the two-way ANOVA. Serum neratinib was compared by repeated measures two-way ANOVA. Diarrhea proportions were analyzed by Chi-squared test. *P* values less than 0.05 were considered statistically significant.

Results

Budesonide co-treatment inhibited growth of rats

Budesonide co-treatment with neratinib was associated with substantial inhibition of growth (Fig. 1). Rats gained significantly less weight (compared to neratinib alone rats), with budesonide rats significantly lighter from day 4 onwards ($P=0.0418$). At day 4, budesonide-treated rats had 3.3% weight loss compared to baseline. The average total weight gained over the 4 weeks of treatment was 15% for budesonide compared to 44% for neratinib alone. Colesevelam co-treatment did not cause any changes to weight gain compared to neratinib treatment alone.

Budesonide- and colesevelam-reduced diarrhea

Rats were assessed each day to determine overall incidence of diarrhea. 50% of rats treated with vehicle control developed diarrhea over the treatment course, however, 37.5% of this was mild diarrhea which occurred on 1 day only, such that it may have been a stress response to the oral gavage procedure, or the vehicle components. Neratinib induced diarrhea in 100% of rats, of which

6.25% was severe diarrhea. No rat co-treated with budesonide or colesevelam developed severe diarrhea. As determined by Chi-squared testing, there was no overall change in diarrhea proportions between groups, however, budesonide ($P=0.027$) and colesevelam ($P=0.033$) significantly decreased the mean number of days with moderate (grade 2) diarrhea (budesonide: 10.0 ± 1 days, colesevelam: 10.0 ± 2.1 days) compared to neratinib alone (15.75 ± 2.7 days) (Fig. 1).

Diarrhea was unrelated to serum neratinib concentration

To assess if the interventions were altering serum absorption of neratinib, systemic neratinib levels were analyzed using mass spectrometry. Serum samples taken from the tail vein after each week of treatment were used. The mean serum concentration of neratinib-treated rats over the entire treatment period was 555.1 ± 36.29 ng/ml. Budesonide or colesevelam did not cause a significant difference to the concentration of neratinib at any time point ($P > 0.05$) (Fig. 2).

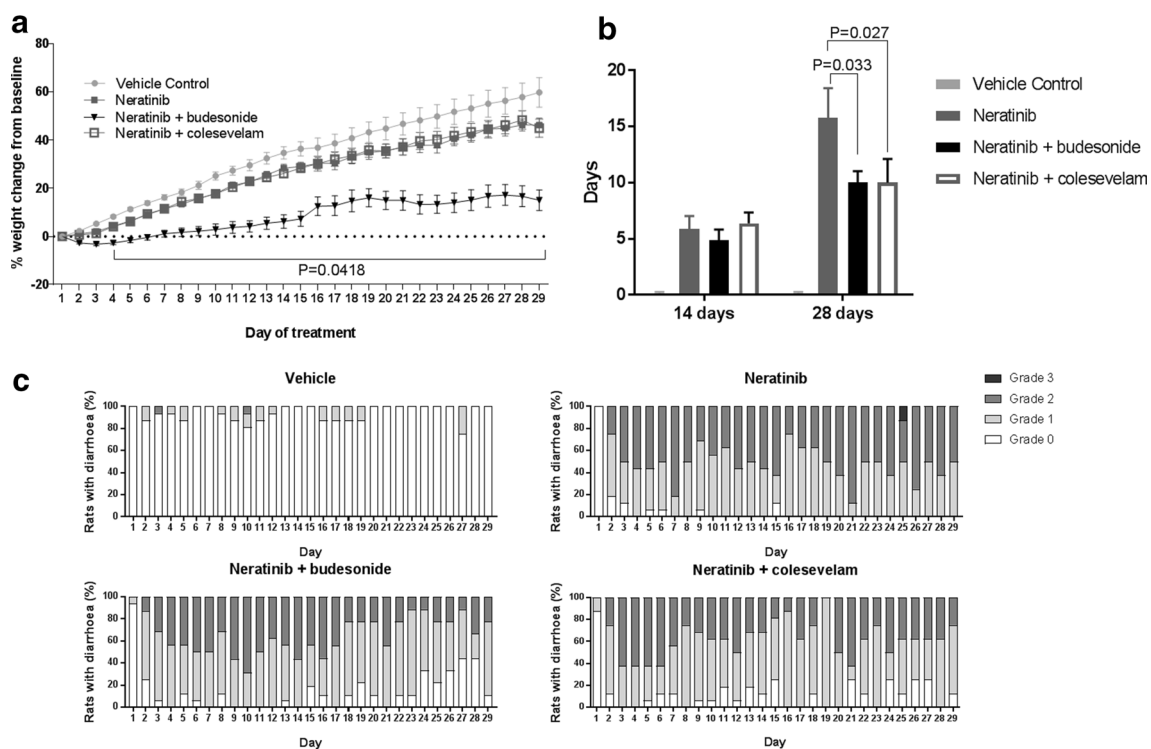


Fig. 1 **a** Body weight change. Data shown as mean \pm SEM. * $P=0.0418$ determined by two-way ANOVA with Dunnett's multiple comparison test. **b** Days with moderate diarrhea. Data shown as mean \pm SEM. Significance determined by two-way ANOVA with

Dunnett's multiple comparisons test. P value is given where significant. **c** Diarrhea severity on each treatment day. Data shown as percentage of total rats

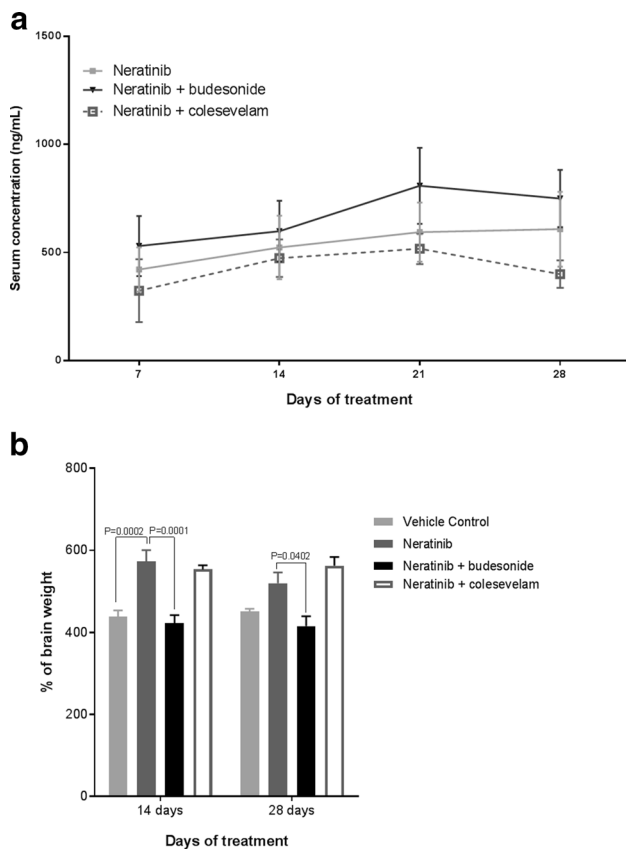


Fig. 2 **a** Serum neratinib concentration determined by liquid chromatography—mass spectrometry. C_{min} shown. Repeated measures data assessed by two-way ANOVA, presented as mean \pm SEM ($n=18$). **b** Small intestinal wet weight following neratinib treatment. Budesonide significantly decreased weight compared to neratinib alone. Data shown as mean \pm SEM. P value is given where significant. Significance determined by two-way ANOVA with Dunnett's multiple comparisons test

Budesonide caused changes to serum biochemistry compared to neratinib alone

Compared to control, neratinib caused a significant increase in serum sodium concentration (14 days, $P=0.0369$), which was prevented by both budesonide and colesevelam. Neratinib also caused an increase in serum urate (28 days, $P=0.0266$) which was prevented by budesonide and colesevelam. ALT was increased in neratinib rats compared to control (14 days, $P=0.0032$), which was prevented by budesonide co-treatment. All other parameters were not significantly different from control (Online Resource 1).

Budesonide decreased a neratinib-induced increase in small intestinal weight

Neratinib caused an increase in small intestinal wet weight (normalized to brain weight) at 14 days from controls

($P=0.0002$). Budesonide administration was able to prevent this ($P=0.0001$). Budesonide also caused a significant decrease in small intestinal weight at the 28 day time point, compared to neratinib alone ($P=0.0402$). Colesevelam did not cause changes to small intestinal weight relative to neratinib alone (Fig. 2).

Budesonide co-treatment modestly protected against histopathological changes

Histopathological changes in neratinib-treated rats mainly consisted of blunting of the villi and inflammatory infiltrate in the lamina propria. After 28 days of treatment, in the distal ileum ($P\leq 0.0001$), proximal colon ($P\leq 0.0001$), and distal colon ($P=0.003$) neratinib-treated rats had significantly higher levels of damage than control animals. There were no significant changes in damage levels in the proximal ileum. Budesonide treated rats had significantly less damage than neratinib alone treated rats in the proximal colon ($P=0.0401$) and distal colon ($P=0.027$). Colesevelam did not cause any statistically significant changes in histopathology when compared to neratinib alone (Fig. 3).

Neratinib and budesonide caused changes in ErbB expression in the ileum

ErbB1, 2 and 4 and ENaC- γ transcript expression was evaluated using RT-PCR (Fig. 4). After 14 days in the ileum, budesonide ($P=0.0180$) and colesevelam ($P=0.0029$) treated groups had significantly lower levels of ErbB1 compared to untreated controls. Neratinib also caused a decrease in ErbB1 transcript compared to controls, although this did not reach significance. ErbB4 expression was decreased in the ileum at 28 days by budesonide treatment ($P=0.042$). Colesevelam was not tested for ErbB4. ErbB2 expression was not significantly changed in any group in the ileum (data not shown). In the colon, there was no significant change in ErbB1, ErbB2 or ErbB4 following neratinib (data not shown). To test if channels involved in sodium absorption in the colon were affected by neratinib we examined relative ENaC- γ mRNA expression. There were no differences between any groups (data not shown).

We also measured total protein expression of ErbB1 by Western blot (Fig. 4). Budesonide ($P=0.0021$) co-treatment was associated with increased ErbB1 compared to controls in the distal ileum. Budesonide ($P=0.0014$) co-treatment was associated with increased pErbB1 (Y1068) compared to controls in the distal ileum. Budesonide ($P=0.0025$) co-treatment was associated with increased pErbB1 compared to neratinib alone in the proximal colon.

The relative expression of pErbB2 in breast cancer is able to dictate sensitivity to targeted agents. Therefore, we used immunohistochemistry in the distal ileum and proximal

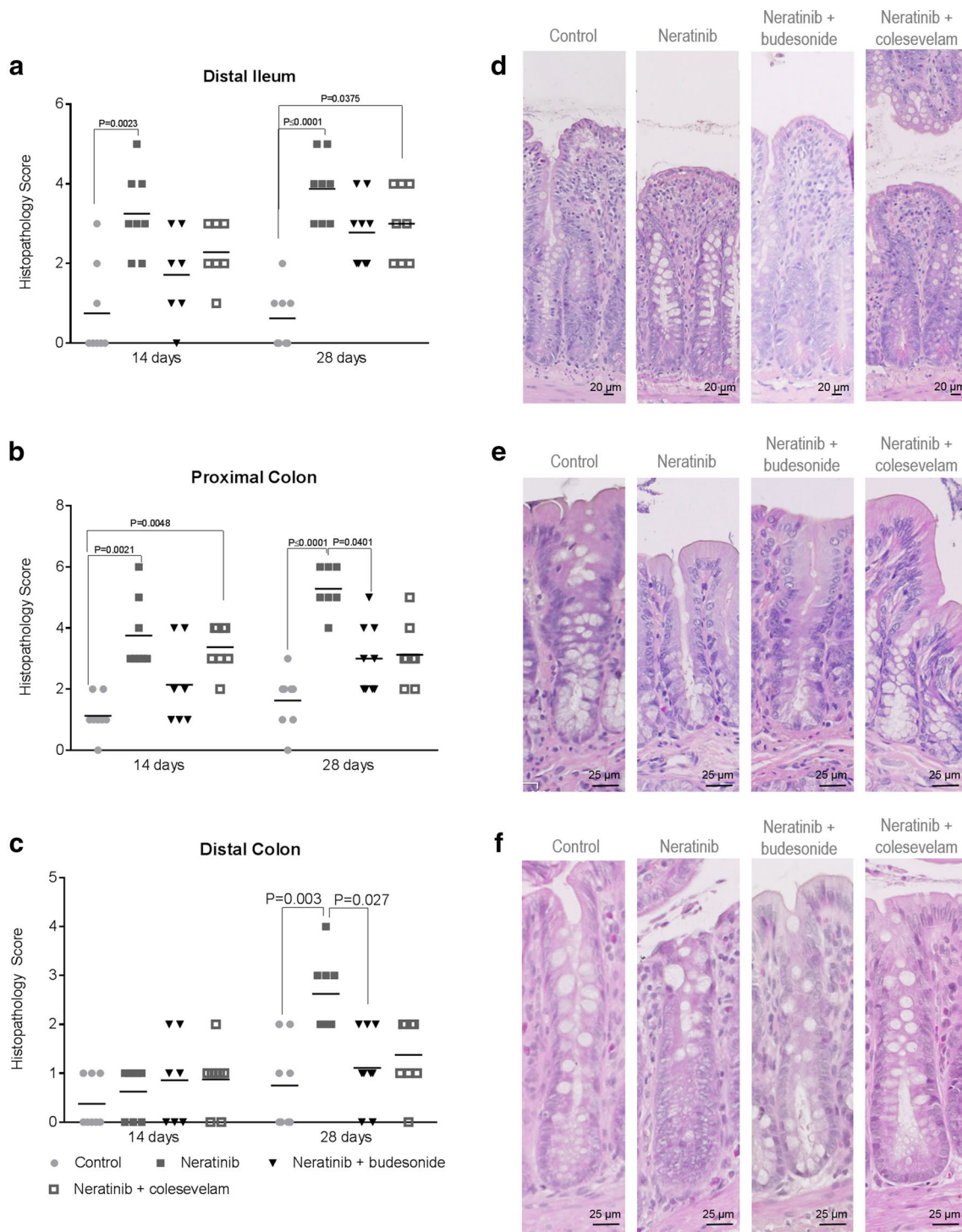


Fig. 3 Neratinib-induced changes in histopathological injury score. **a, d** Distal ileum, **b, e** proximal colon, and **c, f** distal colon. Data shown as mean with scatter. A Kruskal–Wallis test with Dunn’s multiple comparison test was used to determine statistical significance. Repre-

sentative images of hematoxylin and eosin staining at 28 days: original magnification is 200x; scale bars represent 20 or 25 μm as shown in images. *P* value is given where significant

colon to examine tissue expression of pERbB2. Expression was highest in the cell membrane of basal crypt epithelium. The relative expression decreased in rats treated with

neratinib. This was partially prevented by budesonide. This interpretation is by subjective visualization. Representative images in Fig. 5.

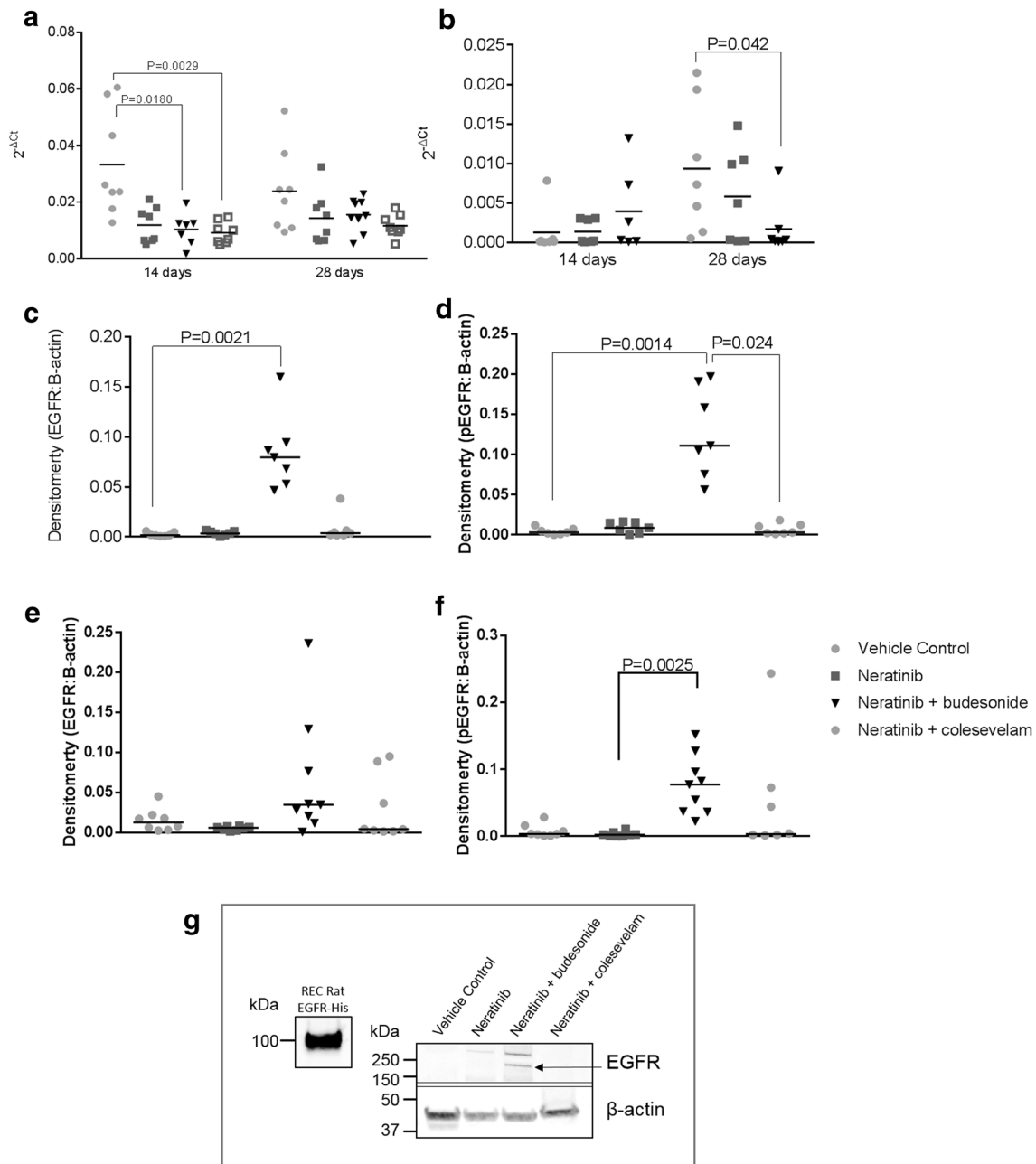


Fig. 4 Changes in ErbB expression measured using Western blot and RT-PCR. **a** Ileum ErbB1 RT-PCR, **b** ileum ErbB4 RT-PCR, **c** Distal ileum ErbB1 western blot, **d** Distal ileum pErbB1 western blot, **e** Proximal colon ErbB1 western blot, **f** Proximal colon pErbB1 western blot, **g** Representative western blot images. Kruskal–Wallis tests

with Dunn's multiple comparisons testing were used to determine statistical significance. Budesonide caused a decrease in ErbB1 mRNA levels in the distal ileum, however, caused an increase in protein ErbB1 levels. *P* value is given where significant

Colesevelam caused an increase in fecal bile acids

Total bile acids were measured in pooled fecal samples collected over 8 h (Fig. 5). There was no change between control and neratinib. Colesevelam caused an increase in bile acids from controls ($P = 0.0026$) and from neratinib

alone ($P = 0.0114$). This is consistent with the pharmacologic action of colesevelam.

As budesonide showed the most effective activity in this model, we further explored the mechanism of protection in those animals. The following assays do not include colesevelam-treated rats.

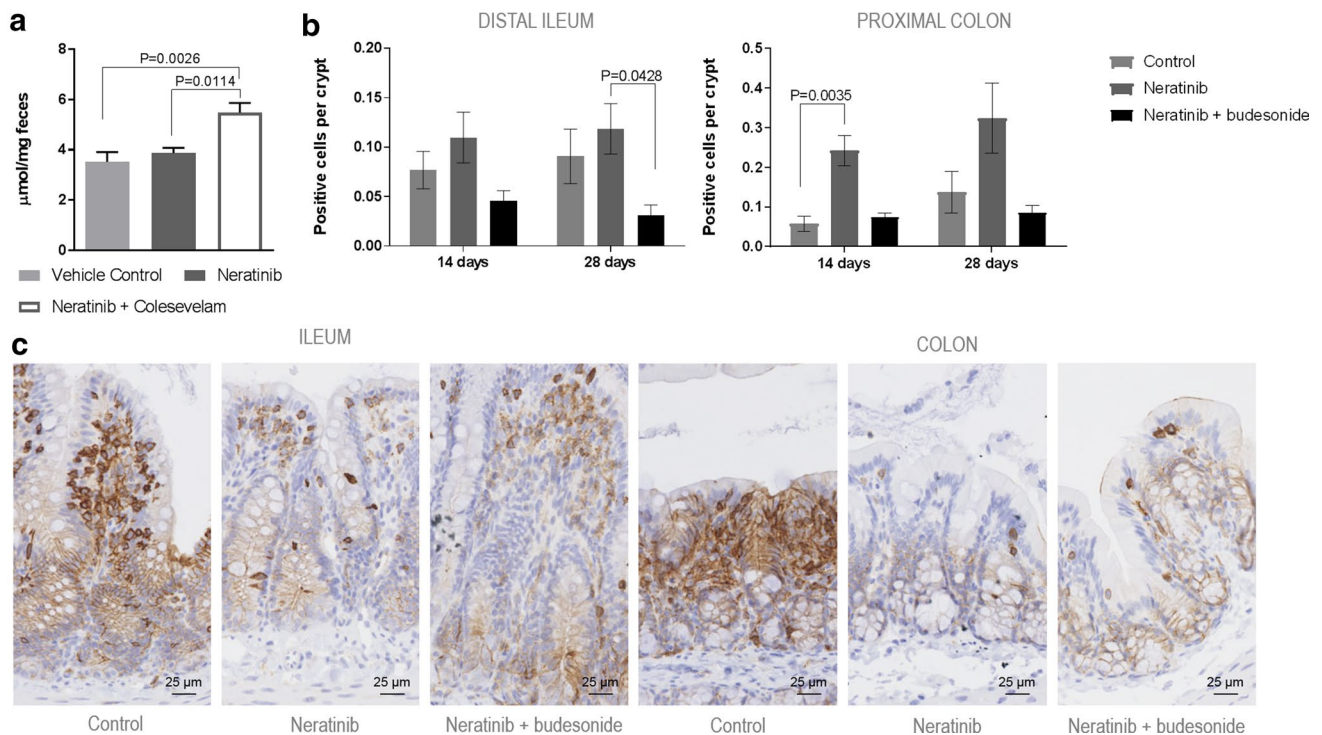


Fig. 5 **a** Colesevelam caused an increase in fecal bile acids in vehicle control animals and in neratinib-treated animals. A one-way ANOVA with Bonferroni post hoc test was used to determine statistical significance. *P* value is given where significant. **b** Levels of caspase-3 positively stained cells in the distal ileum and proximal colon after neratinib treatment. Data shown as mean \pm SEM. A two-way ANOVA

with post hoc test (Bonferroni) was used to determine statistical significance. *P* value is given where significant. **c** Representative images of pErbb2 staining in the distal ileum and proximal colon. Staining was most intense in control animals, with lower staining in neratinib-treated animals. Budesonide partially prevented this change

Neratinib-induced apoptosis in the colon is prevented by budesonide

In the distal ileum after 28 days, rats receiving budesonide had significantly less cleaved caspase-3 positively stained cells than rats receiving neratinib alone ($P=0.0428$) (Fig. 5). After 14 days of treatment, neratinib-treated animals had a fourfold increase in apoptosis in the proximal colon compared to controls ($P=0.0035$). This increase was not seen in budesonide-treated animals.

Budesonide increased anti-inflammatory markers in the ileum and colon

Cytokine levels were measured after 28 days in control, neratinib alone and neratinib + budesonide groups (Fig. 6). Neratinib increased levels of pro-inflammatory IFN- γ in the ileum ($P=0.011$). This significant increase was not seen in budesonide-treated animals. Compared to neratinib alone treated animals, budesonide increased anti-inflammatory IL-4 in ileum ($P=0.0026$) and colon ($P=0.031$) and IL-10 in ileum ($P=0.40$).

Discussion

Neratinib is a promising therapy for HER2+ breast cancer; however, severe diarrhea often associated with treatment has the potential to significantly impact on its clinical usage. This study found that budesonide and colesevelam were able to reduce days with moderate diarrhea in a rat model. In the case of budesonide, this was associated with reduced histopathology score (including inflammatory infiltrate and villus fusion and atrophy) and increased levels of the anti-inflammatory cytokines IL-10 and IL-4, warranting further investigation in clinical trials.

Budesonide caused significantly less weight gain than other groups. This may be of concern in patients who as well as neratinib, may be taking other medications. Animal studies of experimentally induced colitis have shown that budesonide causes weight loss, and at high doses this was enough to prematurely end the experiment [19, 20]. Authors speculated that this weight loss may be due to impairment of gastrointestinal mucosal barrier function, however, as diarrhea was reduced, and glucocorticoids are able to regulate tight junction expression, this does not appear to be the case in this model [20, 21]. Previous models of TKI-induced

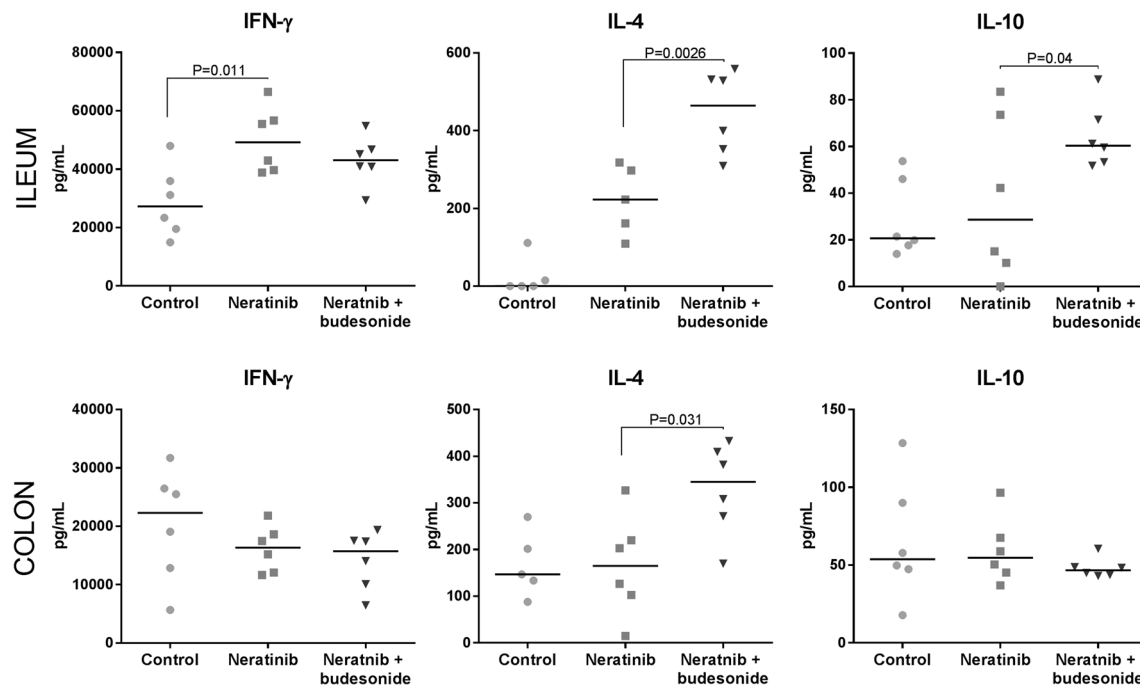


Fig. 6 Cytokine levels after 28 days of neratinib or neratinib + budesonide treatment in the ileum and colon. Data presented as median with scatter. Kruskal–Wallis test with post hoc testing (Dunn’s) used to determine significance. *P* value is given where significant

diarrhea have used changes in apoptosis to assess altered tissue kinetics in gastrointestinal tissue [22]. Budesonide was able to decrease levels of apoptosis in the ileum compared to control. As there was no significant increase in apoptosis due to neratinib treatment alone, apoptotic damage in the small intestine is most likely not a main driver of diarrhea. Additionally, the budesonide-induced decrease in apoptosis is of unclear significance as there was no evidence of major loss of epithelium leading to barrier breakdown. In contrast, neratinib treatment was associated with significantly increased apoptosis in the colon, which was prevented by budesonide. The absolute incidence of crypt cell death was relatively small when contrasted to damage following chemotherapy [17, 23] and so the contribution of apoptotic cell death to the overall pathobiology of neratinib-induced diarrhea is likely to be minimal.

We aimed to better understand the mechanism of neratinib-induced diarrhea to identify potential interventions. From the results of this study, the most prominent histological change was anatomical disruption (characterized by blunting and fusion of villi in the ileum, and disruption and shortening of crypts in the colon). The interventions tested did not completely prevent this, however, budesonide did moderately decrease histopathology score in the colon, and prevented a significant change compared to controls in the ileum. As the jejunum was unaffected, the diarrhea is unlikely to be due to malabsorption of dietary macronutrients in the proximal small intestine. Rather, the results

directed us to focus our attention on the ileum as it is the region of most pronounced neratinib-induced histopathological changes, which impacts on surface area and loss of specialized transporters. Additionally, it has been shown that ErbB1 is expressed at a relatively high level in the ileum compared to the rest of the gastrointestinal tract [22] and may indicate the on-target effects of neratinib are felt greatest in that region.

The interventions used here targeted inflammation and bile acid malabsorption. This was appropriate, as inflammatory infiltrate was seen in the intestines of neratinib-treated rats. Additionally, the brush border of the distal ileum, significantly damaged in this model, contains apical sodium-dependent bile acid transporter (ASBT, SLC10A2), required for active bile acid absorption [24]. Another aspect supporting a role for bile acid malabsorption contributing to neratinib-induced diarrhea in this model is the presence of chronic inflammation in the ileum. It is known that ileitis is associated with decreased bile acid malabsorption through a number of mechanisms. Ileal inflammation is associated with bile acid malabsorption [25], and ASBT expression is decreased in animal models of ileitis [26] and in ileal biopsies from patients with Crohn’s disease [27].

In this study, we measured total fecal bile acids in control, neratinib and neratinib + colestevlam treated groups, and found only significantly increased levels in the colestevlam group, which was expected due to the mode of action of colestevlam. Our interpretation of these results may be

limited, as fasted serum bile acid measurement is more accurate compared to fecal concentration. Despite this, the reduction of diarrhea in rats treated with colesevelam is intriguing, with further research required.

Previous research has suggested a role for altered sodium and chloride transport in the intestine in mediating a secretory form of TKI-induced diarrhea [28]. Additionally, a study in healthy volunteers showed neratinib causes a fecal osmotic gap consistent with values for secretory diarrhea [29]. While the secretory diarrhea hypothesis has been the prevailing hypothesis of this diarrhea mechanism, this is not consistent with the results of our study. We saw no evidence in this study to suggest a role for chloride secretion. After 14 days of treatment, rats treated with neratinib had significantly higher levels of sodium in the serum than control animals, however, the interventions tested did not cause any changes to sodium. Changes in sodium absorption have been well established in models of inflammatory bowel disease related diarrhea [30, 31], and as such, we investigated the induced isoform of the epithelial sodium absorption machinery, in the form of ENaC- γ . We examined relative mRNA expression, and show here that budesonide did not cause changes to ENaC- γ in the colon. However, budesonide also has weak mineralocorticoid activity, which can increase sodium absorption. This occurs because beta and gamma ENaC is upregulated by activation of the mineralocorticoid receptor in the colon. As there were no changes in ENaC- γ , future studies could also consider the role of ENaC- β . The study in healthy volunteers also found inflammatory markers (fecal lactoferrin) in approximately half of the participants with grade 2 diarrhea, supporting our hypothesis that inflammation has a role in neratinib-induced diarrhea [29].

There was a paradoxical effect of budesonide on protein and mRNA levels of ErbB1. While results from Western blot analysis of total protein expression showed an increase compared to controls after 28 days, PCR data showed that budesonide caused lower levels of ErbB1 mRNA compared to controls after 14 days. Further investigation is required to elucidate this finding, which may be dependent on timing of assessment. There is little data available on mechanisms of ErbB transcriptional repression, however, one study found a poor correlation between levels of DNA, RNA and protein in colorectal cancer patients. Additionally, another corticosteroid, dexamethasone, has been shown to increase ErbB1 protein levels in ileal mucosa [32], which supports our findings.

Rats treated with budesonide had significantly higher levels of IL-4 in the ileum and colon compared to rats treated with neratinib alone. IL-4 is an anti-inflammatory cytokine and main partner cell types involved in this process include basophils and eosinophils. Previous research in an asthma model showed that budesonide caused an increase in eosinophil/basophil lineage commitment [33]. Decreased production of IL-4 in inflammatory bowel disease can cause

defective immunosuppressive and anti-inflammatory mechanisms, so a higher level of expression would be expected to diminish intestinal damage [34]. We also show here that budesonide co-treatment led to significantly higher levels of IL-10 in the ileum compared to controls. IL-10 is expressed by a wide variety of T cells and leukocytes such as dendritic cells and neutrophils. It suppresses pro-inflammatory actions of other cells types, and has a key role in inhibiting chronic intestinal inflammation [35]. This increase in IL-10 may be one of the key ways in which budesonide was able to reduce diarrhea via its anti-inflammatory effects. Finally, budesonide prevented the increase in tissue interferon gamma (IFN- γ) following neratinib, complementing our other findings that showed an overall decrease in injury and inflammation in the distal small intestine. There is evidence of IFN- γ increasing intestinal permeability and modulating intestinal epithelial homeostasis, so it is expected that a reduction would lead to less diarrhea [36, 37].

Conclusion

Our study has shown that neratinib-induced diarrhea is multifactorial, encompassing aspects of mucosal inflammation in the distal small intestine. Budesonide and colesevelam were able to reduce levels of diarrhea, and additionally budesonide was able to reduce histopathological injury, and mitigate inflammation. Protection appeared to be via upregulation of anti-inflammatory cytokine production and preservation of intestinal morphology. Clinical studies investigating agents that target these mechanisms are now warranted. This research suggests that in addition to prophylactic loperamide, there may be other targeted agents that may be effective in managing diarrhea in the clinic, and further research is now underway to determine the effectiveness of budesonide and colesevelam in a clinical setting.

Acknowledgements This research was funded by Puma Biotechnology. Dr Janet Collier, Discipline of Pharmacology, University of Adelaide assisted with interpretation of mass spectrometry data. Dr Hannah Wardill, Discipline of Physiology, University of Adelaide, and Dr Ysabella Van Sebille, Division of Health Sciences, University of South Australia assisted with the animal study.

Funding This study was funded by Puma Biotechnology Inc.

Compliance with ethical standards

Conflict of interest Kate Secombe, Imogen Ball, Joseph Shirren, Anthony Wignall and John Finnie declare that they have no conflicts of interest. Joanne Bowen has received research funding from Puma Biotechnology, AstraZeneca, Helsinn and Pfizer. Dorothy Keefe is a consultant for and owns stock in Entrinsic Health Solutions. Francesca Avogadri-Connors, Elizabeth Olek, David Martin and Susan Moran were staff of Puma Biotechnology at the time of the study.

Ethical approval All applicable international, national, and/or institutional guidelines for the care and use of animals were followed. All procedures performed in studies involving animals were in accordance with the ethical standards of the institution or practice at which the studies were conducted. This article does not contain any studies with human participants performed by any of the authors.

References

- Cherian MA, Ma CX (2017) The role of neratinib in HER2-driven breast cancer. *Future Oncol* 13 (22):1931–1943. <https://doi.org/10.2217/fon-2017-0186> (Epub ahead of print)
- Kourie HR, El Rassy E, Clatof F, de Azambuja E, Lambertini M (2017) Emerging treatments for HER2-positive early-stage breast cancer: focus on neratinib. *Onco Targets Ther* 10:3363–3372. <https://doi.org/10.2147/ott.s122397>
- Echavarria I, Lopez-Tarruella S, Marquez-Rodas I, Jerez Y, Martin M (2017) Neratinib for the treatment of HER2-positive early stage breast cancer. *Expert Rev Anticancer Ther* 17(8):669–679. <https://doi.org/10.1080/14737140.2017.1338954>
- Chan A, Delalogue S, Holmes FA, Moy B, Iwata H, Harvey VJ, Robert NJ, Silovski T, Gokmen E, von Minckwitz G, Ejlersen B, Chia SK, Mansi J, Barrios CH, Gnani M, Buysse M, Gore I, Smith J 2nd, Harker G, Masuda N, Petrakova K, Zotano AG, Iannotti N, Rodriguez G, Tassone P, Wong A, Bryce R, Ye Y, Yao B, Martin M (2016) Neratinib after trastuzumab-based adjuvant therapy in patients with HER2-positive breast cancer (ExteNET): a multicentre, randomised, double-blind, placebo-controlled, phase 3 trial. *Lancet Oncol* 17(3):367–377. [https://doi.org/10.1016/s1470-2045\(15\)00551-3](https://doi.org/10.1016/s1470-2045(15)00551-3)
- Park JW, Liu MC, Yee D, Yau C, van 't Veer LJ, Symmans WF, Paoloni M, Perlmutter J, Hylton NM, Hogarth M, DeMichele A, Buxton MB, Chien AJ, Wallace AM, Boughey JC, Haddad TC, Chui SY, Kemmer KA, Kaplan HG, Isaacs C, Nanda R, Tripathy D, Albain KS, Edmiston KK, Elias AD, Northfelt DW, Pusztai L, Moulder SL, Lang JE, Viscusi RK, Euhus DM, Haley BB, Khan QJ, Wood WC, Melisko M, Schwab R, Helsten T, Lyandres J, Davis SE, Hirst GL, Sanil A, Esserman LJ, Berry DA (2016) Adaptive randomization of neratinib in early breast cancer. *N Engl J Med* 375(1):11–22. <https://doi.org/10.1056/NEJMoa1513750>
- Hurvitz S, Chan A, Iannotti N, Ibrahim E, Chien J, Chan N, Kellum A, Hansen V, Marx G, Kendall SD, Wilkinson M, Castrellon A, Ruiz R, Fang P, Hunt D, Moran S, Olek E, Barcenas CH (2017) Rugo HS Effects of adding budesonide or colestipol to loperamide prophylaxis on neratinib-associated diarrhea in patients with HER2 + early-stage breast cancer: the control trial. In: San Antonio Breast Cancer Summit, San Antonio
- McQuade RM, Stojanovska V, Abalo R, Bornstein JC, Nurgali K (2016) Chemotherapy-induced constipation and diarrhea: pathophysiology, current and emerging treatments. *Front Pharmacol* 7:414. <https://doi.org/10.3389/fphar.2016.00414>
- Upadhyay A, Bodar V, Malekzadegan M, Singh S, Frumkin W, Mangla A, Doshi K (2016) Loperamide Induced Life Threatening Ventricular Arrhythmia. *Case Rep Cardiol* 2016:5040176. <https://doi.org/10.1155/2016/5040176>
- Marruffa JM, Holland MG, Sullivan RW, Morgan BW, Oakes JA, Wiegand TJ, Hodgman MJ (2014) Cardiac conduction disturbance after loperamide abuse. *Clin Toxicol (Phila)* 52(9):952–957. <https://doi.org/10.3109/15563650.2014.969371>
- Karthaus M, Ballo H, Abenhardt W, Steinmetz T, Geer T, Schimke J, Braumann D, Behrens R, Behringer D, Kindler M, Messmann H, Boeck HP, Greinwald R, Kleeberg U (2005) Prospective, double-blind, placebo-controlled, multicenter, randomized phase III study with orally administered budesonide for prevention of irinotecan (CPT-11)-induced diarrhea in patients with advanced colorectal cancer. *Oncology* 68(4–6):326–332. <https://doi.org/10.1159/000086971>
- Kwapisz L, Jairath V, Khanna R, Feagan B (2017) Pharmacokinetic drug evaluation of budesonide in the treatment of Crohn's disease. *Expert Opin Drug Metab Toxicol* 13(7):793–801. <https://doi.org/10.1080/17425255.2017.1340454>
- Stein A, Voigt W, Jordan K (2010) Chemotherapy-induced diarrhea: pathophysiology, frequency and guideline-based management. *Ther Adv Med Oncol* 2(1):51–63. <https://doi.org/10.1177/1758834009355164>
- Martinez-Moya P, Ortega-Gonzalez M, Gonzalez R, Anzola A, Ocon B, Hernandez-Chirlaque C, Lopez-Posadas R, Suarez MD, Zarzuelo A, Martinez-Augustin O, Sanchez de Medina F (2012) Exogenous alkaline phosphatase treatment complements endogenous enzyme protection in colonic inflammation and reduces bacterial translocation in rats. *Pharmacol Res* 66(2):144–153. <https://doi.org/10.1016/j.phrs.2012.04.006>
- Beigel F, Teich N, Howaldt S, Lammer F, Maul J, Breitenicher S, Rust C, Goke B, Brand S, Ochsenkuhn T (2014) Colesevelam for the treatment of bile acid malabsorption-associated diarrhea in patients with Crohn's disease: a randomized, double-blind, placebo-controlled study. *J Crohns Colitis* 8(11):1471–1479. <https://doi.org/10.1016/j.crohns.2014.05.009>
- Bowen JM, Mayo BJ, Plews E, Bateman E, Stringer AM, Boyle FM, Finnie JW, Keefe DM (2012) Development of a rat model of oral small molecule receptor tyrosine kinase inhibitor-induced diarrhea. *Cancer Biol Ther* 13(13):1269–1275. <https://doi.org/10.4161/cbt.21783>
- Howarth GS, Francis GL, Cool JC, Xu X, Byard RW, Read LC (1996) Milk growth factors enriched from cheese whey ameliorate intestinal damage by methotrexate when administered orally to rats. *J Nutr* 126(10):2519–2530
- Wardill HR, Gibson RJ, Van Sebille YZ, Secombe KR, Collier JK, White IA, Manavis J, Hutchinson MR, Staikopoulos V, Logan RM, Bowen JM (2016) Irinotecan-induced gastrointestinal dysfunction and pain are mediated by common TLR4-dependent mechanisms. *Mol Cancer Ther* 15(6):1376–1386. <https://doi.org/10.1158/1535-7163.mct-15-0990>
- Boue S, Fortgang I, Levy RJ Jr, Bhatnagar D, Burow M, Fahey G, Heiman ML (2016) A novel gastrointestinal microbiome modulator from soy pods reduces absorption of dietary fat in mice. *Obesity (Silver Spring)* 24(1):87–95. <https://doi.org/10.1002/oby.21197>
- Sann H, Erichsen J, Hessmann M, Pahl A, Hoffmeyer A (2013) Efficacy of drugs used in the treatment of IBD and combinations thereof in acute DSS-induced colitis in mice. *Life Sci* 92(12):708–718. <https://doi.org/10.1016/j.lfs.2013.01.028>
- Ocon B, Aranda CJ, Gamez-Belmonte R, Suarez MD, Zarzuelo A, Martinez-Augustin O, Sanchez de Medina F (2016) The glucocorticoid budesonide has protective and deleterious effects in experimental colitis in mice. *Biochem Pharmacol* 116:73–88. <https://doi.org/10.1016/j.bcp.2016.07.010>
- Fischer A, Gluth M, Weege F, Pape UF, Wiedenmann B, Baumgart DC, Theuring F (2014) Glucocorticoids regulate barrier function and claudin expression in intestinal epithelial cells via MKP-1. *Am J Physiol Gastrointest Liver Physiol* 306(3):G218–G228. <https://doi.org/10.1152/ajpgi.00095.2013>
- Van Sebille YZA, Gibson RJ, Wardill HR, Secombe KR, Ball IA, Keefe DMK, Finnie JW, Bowen JM (2017) Dacomitinib-induced diarrhoea is associated with altered gastrointestinal permeability and disruption in ileal histology in rats. *Int J Cancer J I du Cancer* 140(12):2820–2829. <https://doi.org/10.1002/ijc.30699>
- Gibson RJ, Bowen JM, Cummins AG, Keefe DM (2005) Relationship between dose of methotrexate, apoptosis, p53/p21

- expression and intestinal crypt proliferation in the rat. *Clin Exp Med* 4(4):188–195. <https://doi.org/10.1007/s10238-004-0055-y>
24. Dawson PA, Lan T, Rao A (2009) Bile acid transporters. *J Lipid Res* 50(12):2340–2357. <https://doi.org/10.1194/jlr.R900012-JLR200>
 25. Krag E, Krag B (1976) Regional ileitis (Crohn's disease). I. Kinetics of bile acid absorption in the perfused ileum. *Scand J Gastroenterol* 11(5):481–486
 26. Stelzner M, Somasundaram S, Khakberdiev T (2001) Systemic effects of acute terminal ileitis on uninflamed gut aggravate bile acid malabsorption. *J Surg Res* 99(2):359–364. <https://doi.org/10.1006/jsre.2001.6137>
 27. Jung D, Fantin AC, Scheurer U, Fried M, Kullak-Ublick GA (2004) Human ileal bile acid transporter gene ASBT (SLC10A2) is transactivated by the glucocorticoid receptor. *Gut* 53(1):78–84
 28. Bowen JM (2013) Mechanisms of TKI-induced diarrhea in cancer patients. *Curr Opin Support Palliat Care* 7(2):162–167. <https://doi.org/10.1097/SPC.0b013e32835ec861>
 29. Abbas R, Hug BA, Leister C, Sonnichsen D (2012) A double-blind, randomized, multiple-dose, parallel-group study to characterize the occurrence of diarrhea following two different dosing regimens of neratinib, an irreversible pan-ErbB receptor tyrosine kinase inhibitor. *Cancer Chemother Pharmacol* 70(1):191–199. <https://doi.org/10.1007/s00280-012-1857-3>
 30. Barkas F, Liberopoulos E, Kei A, Elisaf M (2013) Electrolyte and acid-base disorders in inflammatory bowel disease. *Ann Gastroenterol* 26(1):23–28
 31. Priyamvada S, Gomes R, Gill RK, Saksena S, Alrefai WA, Dudeja PK (2015) Mechanisms underlying dysregulation of electrolyte absorption in inflammatory bowel disease-associated diarrhea. *Inflamm Bowel Dis* 21(12):2926–2935. <https://doi.org/10.1097/mib.0000000000000504>
 32. Gordon PV, Price WA, Stiles AD, Rutledge JC (2001) Early postnatal dexamethasone diminishes transforming growth factor alpha localization within the ileal muscularis propria of newborn mice and extremely low-birth-weight infants. *Pediatr Dev Pathol* 4(6):532–537
 33. Cyr MM, Baatjes AJ, Dorman SC, Crawford L, Sehmi R, Foley R, Alam R, Byrne PO, Denburg JA (2008) In vitro effects of budesonide on eosinophil-basophil lineage commitment. *Open Respir Med J* 2:60–66. <https://doi.org/10.2174/1874306400802010060>
 34. West GA, Matsuura T, Levine AD, Klein JS, Fiocchi C (1996) Interleukin 4 in inflammatory bowel disease and mucosal immune reactivity. *Gastroenterology* 110(6):1683–1695
 35. Kole A, Maloy KJ (2014) Control of intestinal inflammation by interleukin-10. *Curr Top Microbiol Immunol* 380:19–38. https://doi.org/10.1007/978-3-662-43492-5_2
 36. Beaurepaire C, Smyth D, McKay DM (2009) Interferon-gamma regulation of intestinal epithelial permeability. *J Interferon Cytokine Res* 29(3):133–144. <https://doi.org/10.1089/jir.2008.0057>
 37. Nava P, Koch S, Laukoetter MG, Lee WY, Kolegraff K, Capaldo CT, Beeman N, Addis C, Gerner-Smidt K, Neumaier I, Skerra A, Li L, Parkos CA, Nusrat A (2010) Interferon-gamma regulates intestinal epithelial homeostasis through converging beta-catenin signaling pathways. *Immunity* 32(3):392–402. <https://doi.org/10.1016/j.immuni.2010.03.001>